



## Higher triplet state of fullerene C70 revealed by electron spin relaxation

Mikhail N. Uvarov, Jan Behrends, and Leonid V. Kulik

Citation: *The Journal of Chemical Physics* **143**, 244314 (2015); doi: 10.1063/1.4938417

View online: <http://dx.doi.org/10.1063/1.4938417>

View Table of Contents: <http://scitation.aip.org/content/aip/journal/jcp/143/24?ver=pdfcov>

Published by the AIP Publishing

---

### Articles you may be interested in

[Electron spin-lattice relaxation of low-symmetry Ni<sup>2+</sup> centers in LiF](#)

*Appl. Phys. Lett.* **104**, 252902 (2014); 10.1063/1.4885381

[Isotropic reorientations of fullerene C70 triplet molecules in solid glassy matrices revealed by light-induced electron paramagnetic resonance](#)

*J. Chem. Phys.* **135**, 054507 (2011); 10.1063/1.3618738

[Spin relaxation of fullerene C70 photoexcited triplet in molecular glasses: Evidence for onset of fast orientational motions of molecules in the matrix near 100 K](#)

*J. Chem. Phys.* **131**, 144501 (2009); 10.1063/1.3244983

[Molecular structure and dynamics of off-center Cu<sup>2+</sup> ions and strongly coupled Cu<sup>2+</sup> – Cu<sup>2+</sup> pairs in BaF<sub>2</sub> crystals: Electron paramagnetic resonance and electron spin relaxation studies](#)

*J. Chem. Phys.* **127**, 124705 (2007); 10.1063/1.2768518

[Electronic structures and dynamics of the excited triplet states of  \$\alpha,\omega\$ -diphenylpolyynes](#)

*J. Chem. Phys.* **114**, 1775 (2001); 10.1063/1.1331614

---



**NEW Special Topic Sections**

**NOW ONLINE**  
Lithium Niobate Properties and Applications:  
Reviews of Emerging Trends

**AIP** Applied Physics Reviews

## Higher triplet state of fullerene C<sub>70</sub> revealed by electron spin relaxation

Mikhail N. Uvarov,<sup>1,a)</sup> Jan Behrends,<sup>2</sup> and Leonid V. Kulik<sup>1,3</sup>

<sup>1</sup>Voevodsky Institute of Chemical Kinetics and Combustion, Siberian Branch of Russian Academy of Sciences, Institutskaya St. 3, 630090 Novosibirsk, Russia

<sup>2</sup>Berlin Joint EPR Lab, Freie Universität Berlin, Arnimallee 14, 14195 Berlin, Germany

<sup>3</sup>Novosibirsk State University, Pirogova St. 2, Novosibirsk, Russia

(Received 7 August 2015; accepted 9 December 2015; published online 29 December 2015)

Spin-lattice relaxation times  $T_1$  of photoexcited triplets  ${}^3\text{C}_{70}$  in glassy decalin were obtained from electron spin echo inversion recovery dependences. In the range 30–100 K, the temperature dependence of  $T_1$  was fitted by the Arrhenius law with an activation energy of  $172\text{ cm}^{-1}$ . This indicates that the dominant relaxation process of  ${}^3\text{C}_{70}$  is described by an Orbach-Aminov mechanism involving the higher triplet state  $t_2$  which lies  $172\text{ cm}^{-1}$  above the lowest triplet state  $t_1$ . Chemical modification of C<sub>70</sub> fullerene not only decreases the intrinsic triplet lifetime by about ten times but also increases  $T_1$  by several orders of magnitude. The reason for this is the presence of a low-lying excited triplet state in  ${}^3\text{C}_{70}$  and its absence in triplet C<sub>70</sub> derivatives. The presence of the higher triplet state in C<sub>70</sub> is in good agreement with the previous results from phosphorescence spectroscopy. © 2015 AIP Publishing LLC. [<http://dx.doi.org/10.1063/1.4938417>]

### I. INTRODUCTION

Fullerenes are promising materials for organic photovoltaic devices and are being used as electron acceptors in the vast majority of organic solar cells.<sup>1</sup> Isolated fullerene molecules can be easily excited to their triplet state by visible light with high quantum yield.<sup>2</sup> While the triplet formation via direct intersystem crossing is usually strongly suppressed when fullerenes are mixed with donor materials, triplet excitons can still affect the photocurrent generated in polymer:fullerene solar cells.<sup>3,4</sup> In particular, the formation of triplet excitons via back electron transfer is a crucial step that can limit the free charge carrier yield and thus the efficiency of organic solar cells.<sup>5–7</sup> Moreover, triplet excitons play a key role in photochemical upconversion<sup>8</sup> and downconversion<sup>9</sup> processes that open the intriguing perspective of increasing the efficiencies of solar cells beyond the Shockley-Queisser limit.<sup>10</sup> These processes critically depend on the excited state dynamics and, in particular, the formation and dissociation probabilities of photoexcited triplet states. An in-depth understanding of both loss mechanisms as well as up- and downconversion processes thus requires detailed knowledge about the triplet state dynamics, including the spin relaxation times and the underlying relaxation mechanisms. Triplet excitons can be observed in the active layer of organic photovoltaic cells by EPR techniques.<sup>11</sup>

Fullerene C<sub>70</sub> and its derivatives are commonly used as acceptor materials in high-efficiency organic solar cells because C<sub>70</sub> based materials have a stronger optical absorption in the visible spectrum than C<sub>60</sub> derivatives.<sup>12</sup>

The triplet intrinsic lifetimes  $\tau_T$  of  ${}^3\text{C}_{70}$  in solutions at room temperatures were obtained as  $\tau_T = 12\text{ ms}$ <sup>13</sup> and  $\tau_T = 24.5\text{ ms}$ <sup>14</sup> which are about one to two orders of magnitude longer than the lifetimes of triplet C<sub>70</sub> derivatives such as 1,2-C<sub>70</sub>H<sub>2</sub> ( $\tau_T = 1.95\text{ ms}$ )<sup>14</sup> and [6,6]-phenyl-C<sub>71</sub>-butyric acid methyl ester, PC<sub>70</sub>BM ( $\tau_T = 140\text{ }\mu\text{s}$ ).<sup>15</sup> At a temperature of 77 K, a triplet lifetime of  ${}^3\text{C}_{70}$  was determined as  $\tau_T = 55\text{ ms}$ <sup>16</sup> and  $\tau_T = 47\text{ ms}$ .<sup>17</sup>

The research interest in  ${}^3\text{C}_{70}$  is also caused by contradictive literature data about its molecular dynamics and spectroscopic features. In a series of works,  ${}^3\text{C}_{70}$  in glassy matrices had been investigated by electron spin echo (ESE)<sup>18–20</sup> and continuous wave (CW) EPR spectroscopy techniques.<sup>16,21–27</sup> The temperature change of the  ${}^3\text{C}_{70}$  EPR line shape was observed by Closs *et al.* for the first time.<sup>21</sup> Later, Terazima *et al.* and Agostini *et al.* suggested that the temperature change of the EPR line shape occurs due to pseudorotations of  ${}^3\text{C}_{70}$  molecules around their larger symmetry axis with correlation times of  $\tau_c \sim 10^{-7}$ – $10^{-6}\text{ s}$  and an activation energy of  $250\text{ cm}^{-1}$ <sup>22</sup> and  $210\text{ cm}^{-1}$ .<sup>24</sup> Levanon *et al.* analyzed the time-resolved EPR line shape of  ${}^3\text{C}_{70}$  in glassy toluene using the model of the pseudorotations with  $\tau_c \sim 10^{-7}\text{ s}$  at temperatures 8 K–114 K, and the presence of two types of  ${}^3\text{C}_{70}$  triplets with different spin-lattice relaxation (SLR) times  $T_1$  of  $0.6\text{ }\mu\text{s}$  and  $5\text{ }\mu\text{s}$  was assumed.<sup>23</sup> The model of one triplet was used to simulate the transient EPR line shape at 114 K and below the toluene melting point.<sup>23</sup> Recently, the CW EPR line shape of  ${}^3\text{C}_{70}$  at 70 K was simulated using a distribution of zero-field splitting (ZFS) parameters  $D$  and  $E$  within an ensemble of frozen  ${}^3\text{C}_{70}$ .<sup>25</sup> One feature in the center of the echo-detected (ED) EPR spectrum of  ${}^3\text{C}_{70}$  appears in the case when the transition energies between the spin sublevels  $|+1\rangle \leftrightarrow |0\rangle$  and  $|0\rangle \leftrightarrow |-1\rangle$  are equal.<sup>20</sup> This feature can manifest itself as a narrow hole or as a spike in the center of ED EPR spectrum depending on turning angles of microwave

<sup>a)</sup>Author to whom correspondence should be addressed. Electronic mail: uvarov@kinetics.nsc.ru. Telephone: +7-383-3332297. Fax: +7-383-3307350.

pulses. It originates from simultaneous excitation of both allowed EPR transitions in  $^3\text{C}_{70}$  by these pulses.

The mechanism of SLR of  $^3\text{C}_{70}$  is not explained up to now. Dauw *et al.* obtained ESE decays of  $^3\text{C}_{70}$  in toluene at 1.2 K. From these data, a SLR time of  $T_1 > 30$  ms was estimated.<sup>18</sup> There were some  $T_1$  measurements of  $^3\text{C}_{70}$  by time-resolved EPR techniques,<sup>23,27</sup> but they are in conflict with more reliable  $T_1$  data obtained by ESE. Further, it was shown that molecular orientations of  $^3\text{C}_{70}$  with non-equilibrium populations of triplet sublevels affect the SLR properties.<sup>18,23,27</sup>

In the present work, SLR times were measured for thermalized  $^3\text{C}_{70}$  in glassy decalin by the ESE inversion recovery technique at temperatures between 20 and 100 K. The aim of this work was to reveal the SLR mechanism of  $^3\text{C}_{70}$ . We found that the exponential dependence of the  $^3\text{C}_{70}$  SLR rate on the inverse temperature can be explained by the presence of a higher triplet state of  $\text{C}_{70}$  with an energy close to the lowest triplet state of  $\text{C}_{70}$ . This makes the Orbach-Aminov mechanism<sup>28,29</sup> the most effective SLR mechanism for  $^3\text{C}_{70}$  in temperature range between 30 and 100 K.

## II. EXPERIMENT

Fullerene  $\text{C}_{70}$  (Aldrich, 99% purity) or [6,6]-phenyl  $\text{C}_{71}$  butyric acid methyl ester (PC<sub>70</sub>BM, Aldrich, 99% purity) were dissolved at a concentration about  $3 \cdot 10^{-4}$  M in decalin (1:1 mixture of *cis*- and *trans*-decalin, Sigma-Aldrich). The samples were put into quartz tubes of 4.6 mm (X-band) or 2.9 mm (Q-band) outer diameter and were frozen in liquid nitrogen to obtain transparent glasses.

Measurements were carried out on ELEXSYS ESP-580E EPR spectrometers equipped with X- or Q-band bridges. For X-band measurements, we used a Bruker ER 4118 X-MD-5 dielectric cavity inside an Oxford Instruments CF 935 cryostat. The temperature was adjusted by a cold nitrogen or helium gas flow and controlled by temperature controllers ER 4131VT or CF 935. For pulse Q-band measurements, we used a laboratory-built cavity in combination with a Bruker Elexsys E-580 pulse EPR spectrometer equipped with a helium flow cryostat.

Electron spin echo signals were obtained as a function of the magnetic field, yielding the so-called ED EPR spectrum. To obtain the echo signal, a two-pulse mw pulse sequence was used (Fig. 1(a)), where the  $\pi/2$  and  $\pi$  pulses were of 40 ns and 80 ns length, respectively. The  $\tau$  delay was 300 ns, and the initial  $T_d$  delay was 600 ns for Q-band. ESE inversion recovery dependences were obtained in X- and Q-bands using a three-pulse sequence with a variation of  $T_d$  (Fig. 1(b)). The experiments of magnetization transfer were carried out on an X-band EPR spectrometer using three-pulse sequence with two different microwave frequencies (Fig. 1(c)). In all experiments in X-band, the lengths of the  $\pi/2$  and  $\pi$  pulses were 16 ns and 32 ns, respectively, the  $\tau$  delay was 120 ns, and the initial  $T_d$  value was 300 ns.

For sample photoexcitation, we used continuous irradiation from an actinic lamp. The estimated light power reaching the sample was about 10 mW. In the pulse EPR experiment, no dark signal was detected.

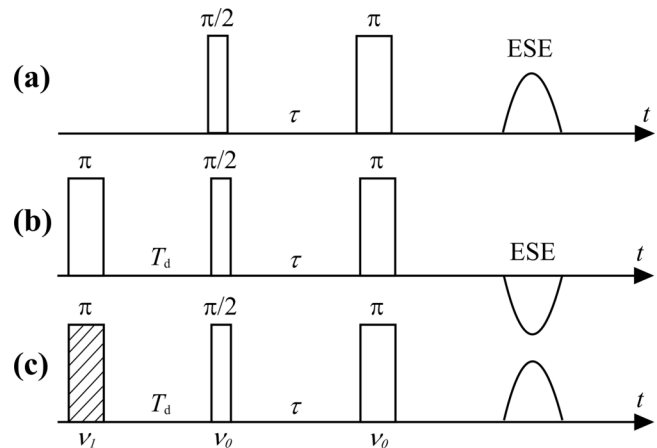


FIG. 1. Microwave pulse sequences which were applied for the experiments of ESE detection (a), ESE inversion-recovery (b), and two-frequency magnetization transfer (c).

Simulations were performed using the MATLAB 6.5 package (The MathWorks, Natick, MA).

## III. THEORY OF ESE INVERSION RECOVERY KINETICS FOR TRIPLET MOLECULES

Assuming that the SLR time is much shorter than the triplet decay time (for  $^3\text{C}_{70}$  it is true at least at temperatures higher than 30 K), the relaxation between the triplet sublevels occurs due to SLR between adjacent spin sublevels  $|+1\rangle \leftrightarrow |0\rangle$  and  $|0\rangle \leftrightarrow |-1\rangle$  with populations  $p_{|+1\rangle}$ ,  $p_{|0\rangle}$ , and  $p_{|-1\rangle}$ , and their sum is constant  $P_0 = p_{|+1\rangle} + p_{|0\rangle} + p_{|-1\rangle} = 1$ . Double quantum relaxation is neglected. The kinetic equations for the populations are<sup>30</sup>

$$\begin{cases} \frac{dp_{|+1\rangle}}{dt} = -w_{|+1,0\rangle}p_{|+1\rangle} + w_{|0,+1\rangle}p_{|0\rangle} \\ \frac{dp_{|0\rangle}}{dt} = -(w_{|0,+1\rangle} + w_{|0,-1\rangle})p_{|0\rangle} + w_{|+1,0\rangle}p_{|+1\rangle} + w_{|-1,0\rangle}p_{|-1\rangle} \\ \frac{dp_{|-1\rangle}}{dt} = -w_{|-1,0\rangle}p_{|-1\rangle} + w_{|0,-1\rangle}p_{|0\rangle} \end{cases}$$

where  $w_{|i,j\rangle}$  are the SLR rates from triplet sublevels  $i$  to  $j$ . Because the Zeeman splitting is much larger than the  $^3\text{C}_{70}$  zero field splitting parameters, the relaxation transition rates between  $|+1\rangle \leftrightarrow |0\rangle$  and  $|0\rangle \leftrightarrow |-1\rangle$  are equal:  $w_{|+1,0\rangle} = w_{|0,-1\rangle}$  and  $w_{|0,+1\rangle} = w_{|-1,0\rangle}$ . The relation between relaxation rates up and down is determined by the Boltzmann factor  $B = \exp(-E_{|i,j\rangle}/kT)$ ,  $w_{|-1,0\rangle} = B w_{|0,-1\rangle}$ ,  $w_{|0,+1\rangle} = B w_{|+1,0\rangle}$  where  $E_{|i,j\rangle}$  denotes the Zeeman splitting between adjacent spin sublevels,  $k$  is the Boltzmann constant, and  $T$  is the temperature.

It is easy to derive that the triplet polarizations  $p_+ = p_{|+1\rangle} - p_{|0\rangle}$  and  $p_- = p_{|-1\rangle} - p_{|0\rangle}$  obey the following equations:

$$\begin{cases} \frac{dp_+}{dt} = -\frac{w}{3}((5+B)p_+ + (1-4B)p_-) + \frac{1}{3}(1-B) \\ \frac{dp_-}{dt} = -\frac{w}{3}((B-4)p_+ + (1+5B)p_-) + \frac{1}{3}(1-B) \end{cases}, \quad (1)$$

where  $w = w_{|+1,0\rangle} = w_{|0,-1\rangle}$ .

In the case of X- and Q-bands EPR measurements, the Boltzmann factor is very close to unity, for example,

$B = 0.96$  for Q-band at 40 K. The equilibrium polarization is  $p_+ = p_- = \delta \equiv (1 - B)/3$ . If the first  $\pi$ -pulse is ideal, it inverts the  $p_+$  polarization from  $\delta$  to  $-\delta$  and does not affect the other allowed EPR transition. At the same time, the  $p_-$  polarization changes from  $\delta$  to  $2\delta$ . The polarization kinetics  $p_+(t)$  and  $p_-(t)$  are the solution of Equations (1) with  $w = 1/T_1$ ,

$$p_+(t) = \delta \left( 1 - \frac{3}{2} \exp(-3t/T_1) - \frac{1}{2} \exp(-t/T_1) \right), \quad (2)$$

$$p_-(t) = \delta \left( 1 + \frac{3}{2} \exp(-3t/T_1) - \frac{1}{2} \exp(-t/T_1) \right). \quad (3)$$

Because the low-field ESE intensity of  $^3\text{C}_{70}$  is proportional to the  $p_+$  polarization (we consider that  $D > 0$  for  $^3\text{C}_{70}$  like it was obtained by Dauw *et al.*<sup>31</sup>), the ESE inversion recovery trace can be fitted by Equation (2) and the SLR time constant  $T_1$  can be obtained. Note that in the described kinetic scheme two-quantum relaxation  $|-1\rangle \leftrightarrow |+1\rangle$  is neglected because all experimental kinetics of inversion-recovery and magnetization transfer experiments were successfully simulated by Eqs. (2) and (3) using the single parameter  $T_1$ . Including the rate of double-quantum relaxation  $W_2$  into the initial kinetic equations leads to a modification of the last exponential terms in Eqs. (2) and (3):  $\exp(-t/T_1)$  will be replaced by  $\exp(-t/T_1 - 2W_2t)$  which will reduce the difference between the expected times of the biexponential inversion-recovery dependences.

Note that in the work of Saal *et al.* the kinetic theory of triplet  $\text{C}_{70}$  was derived to describe phosphorescence kinetics in the absence of a magnetic field.<sup>17</sup> This theory is quite complicated because it involves not only SLR mechanism but also different decay times of the triplet sublevels. This indirect method allowed an estimation of  $T_1 < 10^{-3}$  s for  $^3\text{C}_{70}$  in glassy toluene at 77 K.<sup>17</sup>

## IV. RESULTS AND DISCUSSION

### A. ED EPR spectra of $^3\text{C}_{70}$

Q-band ED EPR spectra of  $^3\text{C}_{70}$  in decalin (Fig. 2(a)) exhibit a line shape similar to X-band ED EPR spectra obtained at the same temperatures.<sup>20</sup> The line shape of ED EPR spectra at 40-90 K could be simulated numerically within the frame of the model suggested in Refs. 20 and 25 (Fig. 2(b)). This model assumes a distribution of ZFS parameters  $D$  and  $E$  within an ensemble of  $^3\text{C}_{70}$  molecules. From these simulations, we can conclude that the outer edges of the ED EPR spectrum correspond to the molecular  $Z$ -axis (the distribution of the  $D$  value is quite small, its width is  $\Delta D = 1.6$  G) but the  $X$ - and  $Y$ -positions are broadened significantly due to a broad distribution of  $E$ -values. The characteristic  $X$ -,  $Y$ -, and  $Z$ -positions of the ED EPR spectrum for two allowed transitions between the  $|+1\rangle \leftrightarrow |0\rangle$  and  $|0\rangle \leftrightarrow |-1\rangle$  spin sublevels are marked in Fig. 2(b). The numerical simulation of the ED EPR spectra of  $^3\text{C}_{70}$  in a broad temperature range is quite complicated because of several reasons. One of them is a strong orientation dependence of the SLR and transverse relaxation rate. At the  $Z$ -positions of ED EPR spectra which corresponds to the molecular  $Z$ -axis of  $^3\text{C}_{70}$  aligned with the direction of the external magnetic field, the SLR is about 5

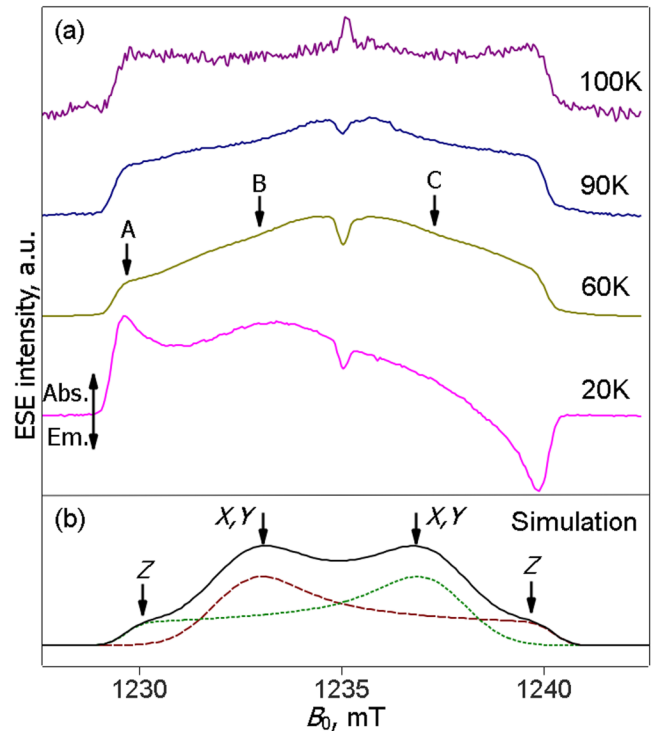


FIG. 2. Echo-detected EPR spectra of  $^3\text{C}_{70}$  in decalin in the temperature range from 20 to 100 K (a). The curves are normalized to the same maximum intensity. The simulation of the mw absorption of frozen  $^3\text{C}_{70}$  molecules in glassy decalin is based on the model of  $D$  and  $E$  value distributions ((b), solid line). The simulated EPR spectrum consists of two contributions from the transitions  $|+1\rangle \leftrightarrow |0\rangle$  ((b), dotted line) and  $|0\rangle \leftrightarrow |-1\rangle$  ((b), dashed line). The calculations were performed using the model and parameters from Ref. 25. A Boltzmann equilibrium within the populations  $p_{|+1\rangle}$ ,  $p_{|0\rangle}$ , and  $p_{|-1\rangle}$  was assumed.

times slower than at the center region of the spectra which corresponds to  $X, Y$ -positions (see Sec. IV B). Because of this reason, the edges of ED EPR spectrum at 100 K are more pronounced. At low temperatures, the ED EPR spectrum becomes polarized: at 20 K, the spectrum contains low-field absorption and high-field emission parts (Fig. 2(a)) because at this temperature the spin-lattice relaxation time is comparable with the triplet lifetime. The narrow feature in the center of the ED EPR spectra originates from the simultaneous excitation of two adjacent triplet spin transitions by mw pulses as explained in Ref. 20.

### B. Spin-lattice relaxation of $^3\text{C}_{70}$

In the temperature range between 20 and 100 K inversion recovery dependences were obtained for A and B spectrum positions corresponding to the  $Z$ - and  $X, Y$ -positions of the ED EPR spectrum (Figs. 2(a) and 2(b)). There is a very strong temperature dependence of the ESE recovery times on the temperature and on the spectral positions (Fig. 3). This raises the question whether only SLR within the triplet spin sublevels determines the ESE inversion recovery dependences or whether spectral diffusion or spin diffusion processes affect this kinetics. It is well-known that a straightforward experiment for measuring SLR times is the ESE saturation recovery experiment in which the processes of spectral and

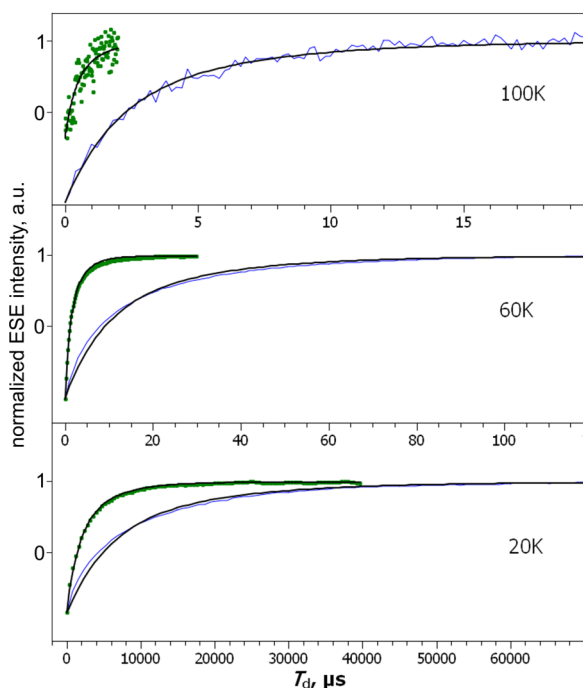


FIG. 3. ESE inversion recovery curves for  ${}^3\text{C}_{70}$  in decalin obtained at the positions A (thin lines) and B (square points) of echo-detected EPR spectrum. Thick lines represent their approximation by biexponential dependences (Eq. (2)).

spin diffusion are suppressed by the first long mw pulse.<sup>32</sup> The dependences of the ESE inversion recovery and ESE saturation recovery (Fig. S2)<sup>40</sup> were found to be very similar and could be fitted by Eq. (2). That is why we concluded that the ESE inversion recovery dependences are characterized only by a SLR process involving the triplet sublevels. Thus, the kinetics of Fig. 3 were approximated by biexponential dependences as given in Eq. (2). However, the ratio of the coefficients between the amplitudes of the two exponential decays was decreased from 3.0 to 1.9. This could be attributed to a non-ideal inversion pulse. Note that no good approximation of the inversion-recovery traces by biexponential dependences could be achieved with the ratio between the time constants of both exponential decays larger than 3. However, if the two-quantum transition noticeably affects the inversion-recovery dependence, this ratio should be smaller than 3, which follows from the above theory of relaxation in a three-level system.

The values of  $T_1$  for the spectral positions A and B of  ${}^3\text{C}_{70}$  are presented in the semilogarithmic plot in Fig. 4. Note that the  $T_1$  values obtained in X-band were very similar to those obtained in Q-band at the identical temperatures (Fig. 4).

At temperatures above 30 K, the temperature dependences of  $T_1$  were fitted by the exponential law

$$1/T_1 = A_p \exp(-E_p/kT),$$

where  $A_p$  is a pre-exponential factor and  $E_p$  is an activation energy. Note that the points of  $T_1^{-1}$  at 20 K deviate from the exponential law because at low temperatures the triplet decay prevails over the SLR process. Pre-exponential factors  $A_A = 2.9 \times 10^6 \text{ s}^{-1}$  and  $A_B = 1.4 \times 10^7 \text{ s}^{-1}$ , and activation energies 22 meV and 20 meV for A and B ED EPR spectral positions, were obtained. This indicates that for  ${}^3\text{C}_{70}$

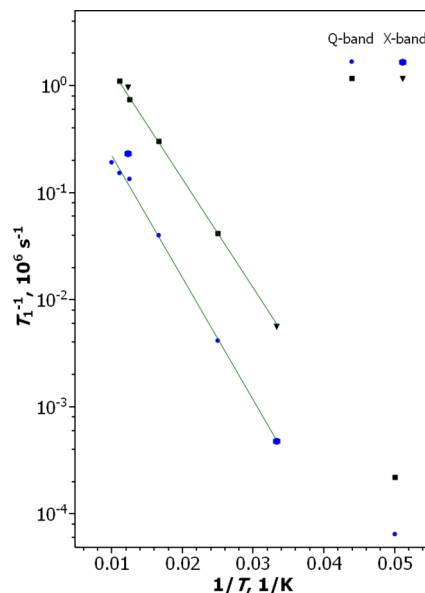


FIG. 4. Temperature dependence of  $T_1$  of  ${}^3\text{C}_{70}$  in decalin obtained in two ED EPR spectrum positions A (circles) and B (squares) at different temperatures in Q-band, and in positions A (hexagon) and B (triangle) in X-band. Lines: the approximations of the  $T_1^{-1}$  by the Orbach-Aminov law with an activation energy of  $172 \text{ cm}^{-1}$ .

the SLR is determined by an Orbach-Aminov relaxation mechanism, since only this mechanism predicts an Arrhenius-type temperature dependence of the SLR rate. The other most effective relaxation mechanism (Raman process) leads to a power dependence of the relaxation rate on the temperature, which allows distinguishing these processes.<sup>33</sup> It is also possible that at low temperatures the contribution of the Orbach-Aminov process to the SLR is small and the contribution from the Raman process becomes substantial. The physical meaning of an Orbach-Aminov SLR mechanism is relaxation through the excited electronic state, in our case the triplet state  $t_2$ , which lies higher than the lowest triplet state  $t_1$ . The energy gap between these states is equal to the activation energy of the SLR process. Its value (averaged over the two spectral positions A and B) is  $E_{t_2} = 21 \text{ meV} = 172 \text{ cm}^{-1}$  for  ${}^3\text{C}_{70}$ . A similar energy gap between the lowest triplet state ( $12\,404 \text{ cm}^{-1}$  above the singlet ground state) and the next triplet state ( $12\,659 \text{ cm}^{-1}$  above the singlet ground state) was extracted from phosphorescence spectra of  $\text{C}_{70}$  in frozen glassy solutions.<sup>34</sup> Moreover, the intensity of the line at  $12\,659 \text{ cm}^{-1}$  (which was called A-band<sup>34</sup>) of the excited triplet state of  $\text{C}_{70}$  in the phosphorescence spectrum increases upon raising the temperature, and this line is observable only at temperatures higher than 70 K.<sup>34</sup> A very similar energy gap of  $165 \text{ cm}^{-1}$  between triplet states with different symmetries ( $A_2'$  for the lowest triplet state and  $E_1'$  for the first excited triplet state) was obtained for  ${}^3\text{C}_{70}$  in a solid neon matrix by means of phosphorescence spectroscopy.<sup>35</sup>

It was found that the pre-exponential factors  $A_A$  and  $A_B$  differ by a factor of 5. This means that the  ${}^3\text{C}_{70}$  molecular orientation affects the rate of the Orbach-Aminov process. The anisotropy of the spin relaxation for  ${}^3\text{C}_{70}$  is not surprising since the  $\text{C}_{70}$  molecule itself is not spherically symmetric. The spin relaxation process depends on the projection of the initial

eigenstates of  $t_1$  on the eigenstates of  $t_2$ . Thus, the smaller SLR rate observed for the Z-position in the ED EPR spectrum might indicate that the orientation of the Z-axis of  ${}^3\text{C}_{70}$  is preserved during  $t_1 \leftrightarrow t_2$  transitions, whereas the direction of the X- and Y-orientations changes noticeably.

In some works,<sup>22–24</sup> pseudorotation around the long  $\text{C}_{70}$  axis was suggested to be the dominant SLR mechanism of  ${}^3\text{C}_{70}$ . However, it is easy to show that it cannot induce such a fast SLR as it was obtained at temperatures around 100 K. Indeed, according to Redfield theory, the SLR rate approximately equals  $1/T_1 = V^2/(1 + \omega_0^2\tau_c^2)$ , where  $V$  is the magnitude of the fluctuating interaction,  $\omega_0$  is Zeeman frequency, and  $\tau_c$  is the correlation time of the fluctuation. This SLR rate has its maximal value  $(1/T_1)_{\text{max}} = V^2/(2\omega_0)$  when  $\omega_0\tau_c = 1$ . For pseudorotations around the long  $\text{C}_{70}$  axis, a magnitude of EPR frequency fluctuation is proportional to the ZFS parameter  $E \approx 2 \times 10^8$  rad/s. For Q-band  $\omega_0 \approx 2 \times 10^{11}$  rad/s, so  $(1/T_1)_{\text{max}} = 10^5 \text{ s}^{-1}$  which is ten times slower than the fastest observed SLR rate for  ${}^3\text{C}_{70}$ . Moreover, the real  $\tau_c$  should be much larger than  $10^{-11} \text{ s}^{-1}$ , because such a fast pseudorotation leads to averaging of the non-axial part of ZFS tensor and axial EPR spectrum, which is not the case for  ${}^3\text{C}_{70}$  at temperatures below 100 K.

### C. Magnetization transfer between ED EPR spectrum positions of ${}^3\text{C}_{70}$

The increase of the polarization  $p_+$  was achieved by inverting the  $p_-$  polarization by a  $\pi$ -pulse in the experiments on magnetization transfer for  ${}^3\text{C}_{70}$  in decalin. A three-pulse mw sequence with two frequencies  $\nu_0$  and  $\nu_1$  was applied (Fig. 1(c)). The difference between  $\nu_0$  and  $\nu_1$  of 70 MHz results in a shift of the resonance position for  $\nu_1$  by 25 G from that of  $\nu_0$ . Thus, a  $\pi$ -pulse with the frequency  $\nu_1$  inverted the spin polarization at the spectral position C whereas the last two pulses with a frequency  $\nu_0$  produced the resonance ESE signal in the spectral position B (Fig. 2). The spectral positions B and C were chosen because they correspond to the transitions  $T_+ \leftrightarrow T_0$ , and  $T_0 \leftrightarrow T_-$  of  ${}^3\text{C}_{70}$  molecules. The preferential orientation of the external magnetic field for these spectral positions is orthogonal to the long  $\text{C}_{70}$  axis, i.e., it corresponds to XY-position of the triplet EPR spectrum.

The dependence of the ESE signal intensity on the delay  $T_d$  in magnetization transfer and inversion recovery experiments is shown in Fig. 5 (at a temperature of 30 K). These traces were fitted by biexponential dependences as given in Eqs. (2) and (3) with  $T_1 = 64 \mu\text{s}$  with the ratio of the amplitudes of the two exponential decays changed to obtain the best fitting. The deviation from the dependences given in Eqs. (2) and (3) is probably caused by the distribution of the  ${}^3\text{C}_{70}$  relaxation time due to its orientation- and site-dependence. Both experiments are consistently described within the SLR model: the same time  $T_1$  is obtained from magnetization transfer and inversion recovery traces. This implies that the evolution of the longitudinal magnetization in  ${}^3\text{C}_{70}$  is governed by true spin-lattice relaxation but by not pseudorotations in microsecond time scale which was suggested in Ref. 22. Our results allow to suggest a new explanation of the evolution time-resolved EPR spectra of  ${}^3\text{C}_{70}$  with an increase of the delay

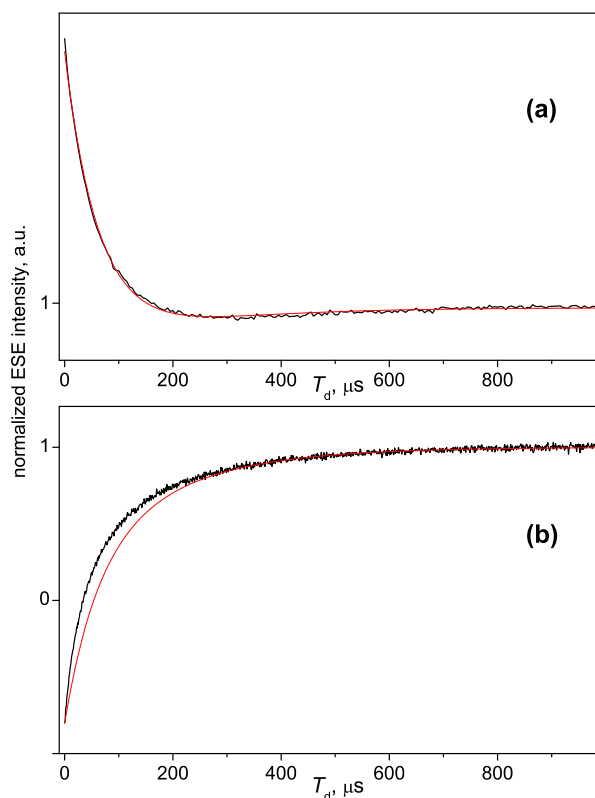


FIG. 5. Dependences of the ESE intensity on the delay  $T_d$  in three-pulse sequences: magnetization transfer (a) and inversion recovery (b). Red lines: approximation of the experimental traces by biexponential dependences. Note that the relative amplitude of the exponential decays differs from that in Eqs. (2) and (3).  ${}^3\text{C}_{70}$  in decalin, X-band, detection in position B of the EPR spectrum, temperature 30 K.

after laser flash (DAF) which were obtained by Terazima *et al.*<sup>22</sup> At the edges of these time-resolved EPR spectra (Z-positions), the lines become more pronounced for long DAF while the features in the center of the spectra disappear. This is caused simply by an anisotropic SLR for  ${}^3\text{C}_{70}$  molecules for which the SLR time for canonical Z-orientations is longer than for the canonical X- and Y-orientations.

The SLR times presented in the present work are in conflict with the results of the work of Levanon *et al.*<sup>23</sup> In that work, the transient EPR spectra and kinetics were simulated with several parameters (the contribution of two triplets was assumed) and unrealistically short SLR times were used to describe the experimental data at 8 K. Our direct measurements of SLR of  ${}^3\text{C}_{70}$  by ESE inversion recovery, ESE saturation recovery, and magnetization transfer revealed the reliable values of SLR times and a very strong temperature dependence of the SLR times.

### D. ED EPR spectra of ${}^3\text{PC}_{70}\text{BM}$ in decalin

To check the influence of a chemical modification of  $\text{C}_{70}$  on the relaxation of the fullerene triplet state, pulse EPR experiments on  ${}^3\text{PC}_{70}\text{BM}$  were carried out. There are three structures of  $\text{PC}_{70}\text{BM}$  isomers with significant contributions.<sup>36</sup> In the work of Franco *et al.*<sup>37</sup> on three triplet isomers of a  $\text{C}_{70}$  derivative (which were not  $\text{PC}_{70}\text{BM}$ ), the EPR line shape was numerically simulated as a sum of three EPR spectra of

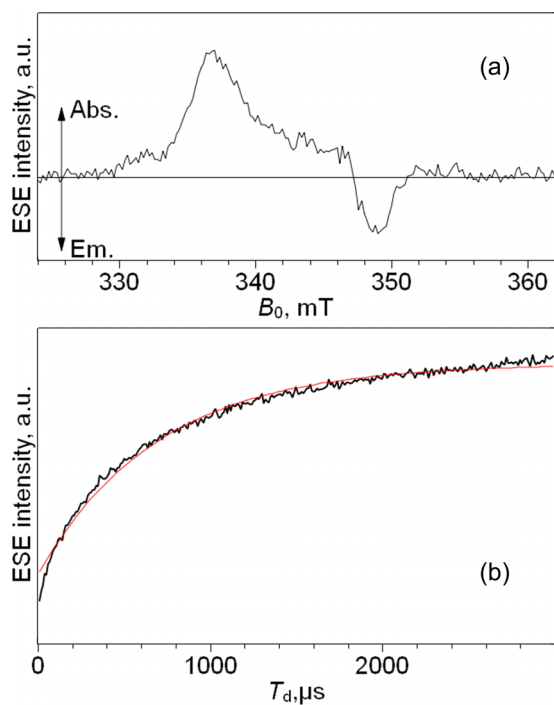


FIG. 6. X-band echo-detected EPR spectrum of the triplet state of  $PC_{70}BM$  in decalin at 80 K (a), and inversion recovery kinetics at the maximum of the ED EPR spectrum ((b), thick line) with an exponential approximation,  $T_1 = 700 \mu s$  ((b), thin line).

three triplets. For a quantitative description of the obtained ED EPR spectrum of triplet molecules  $^3PC_{70}BM$  in decalin at a temperature of 80 K (Fig. 6(a)), a similar approach should be used. The obtained ED EPR spectrum was not simulated due to complexity of its line shape. The emissive part at its high-field region allows an estimation of the SLR time of one of the  $^3PC_{70}BM$  isomers. Such a non-equilibrium polarization for the  $^3C_{70}$  molecules was observed at temperatures lower than 30 K when the triplet lifetime is quite short and the triplet decay occurs faster than thermal equilibrium is established within the triplet spin sublevels.<sup>20</sup> That is why at least one of the  $PC_{70}BM$  isomers has a triplet lifetime less than its apparent ESE recovery time at 80 K. A characteristic time of 700  $\mu s$  was obtained for the ESE inversion recovery dependence of  $^3PC_{70}BM$  at the low field maximum of the ED EPR spectrum at 80 K (Fig. 6(b)). This time is indeed longer than the triplet lifetime of  $^3PC_{70}BM$  of  $\tau_T = 140 \mu s$  measured at room temperature.<sup>15</sup> Overall this shows that the SLR processes in  $^3C_{70}$  and  $^3PC_{70}BM$  are substantially different: SLR of  $^3PC_{70}BM$  is much slower than SLR of  $^3C_{70}$  at 77 K. This SLR of  $^3PC_{70}BM$  could not be described by an Orbach-Aminov relaxation mechanism with an energy comparable to the obtained  $E_{t_2}$ . The reason for this is the absence of a close lying excited electronic state in  $^3PC_{70}BM$ . The difference between  $^3C_{70}$  and  $^3PC_{70}BM$  can be traced back to their electronic structure. Due to its high symmetry,  $C_{70}$  has several molecular orbitals very close in energy<sup>38</sup> which result in several close-lying triplet states of  $C_{70}$  with different symmetries of the electronic wavefunction.<sup>39</sup> This is probably not the case for  $PC_{70}BM$  because its symmetry is reduced.

## V. CONCLUSION

In the temperature range between 20 and 100 K, spin-lattice relaxation times  $T_1$  of  $^3C_{70}$  were obtained from biexponential fitting of ESE inversion recovery curves. They were analytically described by the solution of kinetic equations for the relaxation within the triplet sublevels with the single relaxation time  $T_1$ . The temperature dependence of  $T_1$  was fitted by the Arrhenius law with an activation energy of  $E_{t_2} = 172 \text{ cm}^{-1}$ . This indicates that the dominant relaxation process is Orbach-Aminov spin-lattice relaxation of  $^3C_{70}$  through the higher triplet state  $t_2$  with symmetry  $E'_1$  which lies by the energy  $E_{t_2}$  higher than the primary triplet state  $t_1$  with symmetry  $A'_2$ . Modification of  $C_{70}$  fullerene not only decreases the intrinsic triplet lifetime but also strongly increases the SLR time. The suggested reason for this is the difference in the absence of low-lying triplet excited state in  $C_{70}$  derivatives.

## ACKNOWLEDGMENTS

This work was supported by the Russian Foundation for Basic Research, Grant No. 15-33-20421; the Scholarship of the President of the Russian Federation, Grant No. 3596.2013.1; the Ministry of Education and Science of the Russian Federation; German Academic Exchange Service (DAAD) Scholarship. The authors are thankful to Professor S. A. Dzuba for stimulating discussions.

- <sup>1</sup>S. Kirner, M. Sekita, and D. M. Guldi, *Adv. Mater.* **26**, 1482 (2014).
- <sup>2</sup>J. W. Abrogast, A. P. Darmanyan, C. S. Foote, Y. Rubin, F. N. Diedrich, M. M. Alvarez, S. J. Anz, and R. L. Whetten, *J. Phys. Chem.* **95**, 11 (1991).
- <sup>3</sup>B. Z. Tedlla, F. Zhu, M. Cox, J. Drijkoningen, J. Manca, B. Koopmans, and E. Goovaerts, *Adv. Energy Mater.* **5**, 1401109 (2015).
- <sup>4</sup>B. Z. Tedlla, F. Zhu, M. Cox, B. Koopmans, and E. Goovaerts, *Phys. Rev. B* **91**, 085309 (2015).
- <sup>5</sup>A. Rao, P. C. Y. Chow, S. Gelinas, C. W. Schlenker, C.-Z. Li, H.-L. Yip, A. K.-Y. Jen, D. S. Ginger, and R. H. Friend, *Nature* **500**, 435 (2013).
- <sup>6</sup>A. Distler, P. Kutka, T. Sauermann, H. Egelhaaf, D. M. Guldi, D. D. Nuzzo, S. C. J. Meskers, and R. A. J. Janssen, *Chem. Mater.* **24**, 4397 (2012).
- <sup>7</sup>A. Köhler and H. Bässler, *Mater. Sci. Eng., R* **66**, 71 (2009).
- <sup>8</sup>T. F. Schulze and T. W. Schmidt, *Energy Environ. Sci.* **8**, 103 (2015).
- <sup>9</sup>M. C. Hanna and A. J. Nozik, *J. Appl. Phys.* **100**, 074510 (2006).
- <sup>10</sup>W. Shockley and H. J. Queisser, *J. Appl. Phys.* **32**, 510 (1961).
- <sup>11</sup>F. Kraffert, R. Steyrlleuthner, S. Albrecht, D. Neher, M. C. Scharber, R. Bittl, and J. Behrends, *J. Phys. Chem. C* **118**, 28482 (2014).
- <sup>12</sup>Y. Li, *Acc. Chem. Res.* **45**, 723 (2012).
- <sup>13</sup>K. D. Ausman and R. B. Weisman, *Res. Chem. Intermed.* **23**, 431 (1996).
- <sup>14</sup>S. M. Bachilo, A. F. Benedetto, R. B. Weisman, J. R. Nossal, and W. E. Billups, *J. Phys. Chem. A* **104**, 11265 (2000).
- <sup>15</sup>P. C. Y. Chow, S. Alert-Seifried, S. Gelinas, and R. H. Friend, *Adv. Mater.* **26**, 4851 (2014).
- <sup>16</sup>M. R. Wasielewski, M. P. O'neil, K. R. Lykke, M. J. Pellin, and D. M. Gruen, *J. Am. Chem. Soc.* **113**, 2774 (1991).
- <sup>17</sup>C. Saal, N. Weiden, and K.-P. Dinse, *Appl. Magn. Reson.* **11**, 335 (1996).
- <sup>18</sup>X. L. R. Dauw, O. G. Poluektov, J. B. M. Wartjes, M. V. Bronsveld, and E. J. J. Groenen, *J. Phys. Chem. A* **102**, 3078 (1998).
- <sup>19</sup>M. N. Uvarov, L. V. Kulik, and S. A. Dzuba, *J. Chem. Phys.* **131**, 144501 (2009).
- <sup>20</sup>M. N. Uvarov, L. V. Kulik, T. I. Pichugina, and S. A. Dzuba, *Spectrochim. Acta, Part A* **78**, 1548 (2011).
- <sup>21</sup>G. L. Closs, P. Gautam, D. Zhang, P. J. Krusi, S. A. Hill, and E. Wasserman, *J. Phys. Chem.* **96**, 5228 (1992).
- <sup>22</sup>M. Terazima, K. Sakurada, N. Hirota, H. Shinohara, and Y. Saito, *J. Phys. Chem.* **97**, 5447 (1993).
- <sup>23</sup>H. Levanon, V. Meiklyar, S. Michaeli, and D. Gamliel, *J. Am. Chem. Soc.* **115**, 8722 (1993).
- <sup>24</sup>G. Agostini, C. Corvaja, and L. Pasimeni, *Chem. Phys.* **202**, 349 (1996).

- <sup>25</sup>M. N. Uvarov, L. V. Kulik, and S. A. Dzuba, *Appl. Magn. Reson.* **40**, 489 (2011).
- <sup>26</sup>M. N. Uvarov, L. V. Kulik, A. B. Doktorov, and S. A. Dzuba, *J. Chem. Phys.* **135**, 054507 (2011).
- <sup>27</sup>M. Terazima, N. Hirota, H. Shinohara, and Y. Saito, *Chem. Phys. Lett.* **195**, 333 (1992).
- <sup>28</sup>L. K. Aminov, *Exp. Theor. Phys.* **15**, 547 (1962).
- <sup>29</sup>R. Orbach, *Proc. R. Soc. A* **264**, 458 (1961).
- <sup>30</sup>H. Seidel, M. Mehring, and D. Stehlik, *Chem. Phys. Lett.* **104**, 552 (1984).
- <sup>31</sup>X. L. R. Dauw, J. Visser, and E. J. J. Groenen, *J. Phys. Chem. A* **106**, 3754 (2002).
- <sup>32</sup>A. Schweiger and G. Jeschke, *Principles of Pulse Electron Paramagnetic Resonance* (Oxford University Press, 2001).
- <sup>33</sup>L. Kulik, W. Lubitz, and J. Messinger, *Biochemistry* **44**, 9368 (2005).
- <sup>34</sup>S. M. Argentine, K. T. Kotz, and A. H. Francis, *J. Am. Chem. Soc.* **117**, 11762 (1995).
- <sup>35</sup>A. Sassara, G. Zerza, and M. Chergui, *J. Phys. Chem. A* **102**, 3072 (1998).
- <sup>36</sup>M. M. Wienk, J. M. Kroon, W. J. H. Verhees, J. Knol, J. C. Hummelen, P. A. van Hal, and R. A. J. Janssen, *Angew. Chem., Int. Ed.* **42**, 3371 (2003).
- <sup>37</sup>L. Franco, A. Toffoletti, and M. Maggini, *Phys. Chem. Chem. Phys.* **14**, 14358 (2012).
- <sup>38</sup>G. E. Scuseria, *Chem. Phys. Lett.* **180**, 451 (1991).
- <sup>39</sup>M. van Gastel, *J. Phys. Chem. A* **114**, 10864 (2010).
- <sup>40</sup>See supplementary material at <http://dx.doi.org/10.1063/1.4938417> for the spin-lattice relaxation time measuring by ESE saturation and inversion recovery experiments.